analytical chemistry

Technical Note

pubs.acs.org/ac

Integration of On-Chip Isotachophoresis and Functionalized Hydrogels for Enhanced-Sensitivity Nucleic Acid Detection

Giancarlo Garcia-Schwarz and Juan G. Santiago*

Department of Mechanical Engineering, Stanford University, Stanford, California 94305, United States

Supporting Information

ABSTRACT: We introduce an on-chip electrokinetic assay to perform high-sensitivity nucleic acid (NA) detection. This assay integrates electrokinetic sample focusing using isotachophoresis (ITP) with a background signal-removal strategy that employs photopatterned, DNA-functionalized hydrogels. In this multistage assay, ITP first enhances hybridization kinetics between target NAs and end-labeled complementary reporters. After enhanced hybridization, migration through a DNA-functionalized hydrogel region removes excess reporters through affinity interactions. We demonstrate our assay on microRNAs, an important class of low-abundance biomarkers. The assay exhibits 4 orders of magnitude dynamic range, near 1 pM detection limits starting from less than 100 fg of microRNA, and high selectivity for mature microRNA sequences, all within a 10 min run time. This new microfluidic framework provides a unique quantitative assay for NA detection.

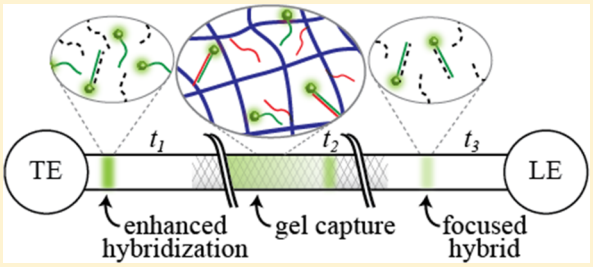

We present an electrokinetic assay which integrates isotachohporesis (ITP) and a photopatterned DNA-functionalized hydrogel for rapid and sensitive nucleic acid (NA) detection. ITP preconcentrates NAs to enhance the hybridization reaction between target molecules and fluorescently-labeled complementary oligonucleotides, which we term reporters. After this reaction, ITP drives products into a DNA-functionalized hydrogel which removes excess unreacted reporters from the focused ITP zone, drastically reducing background signal. Our approach is generally applicable to detection of any NA (e.g., DNA, mRNA, etc.).

We here present detection of synthetic microRNAs as one example quantitative demonstration of our assay. microRNAs are short (~22 nt) noncoding molecules that play an important role in gene silencing within the cell.[1] Dysregulation of microRNA expression has been linked to multiple forms of cancer and is considered an important diagnostic and prognostic signature.[2−5] Absolute quantification of microRNA species presents four main challenges: (1) microRNAs are low in abundance, together making up only about 0.1% (w/w) of a cell's total RNA content,[6] (2) concentrations of a single microRNA species can vary by over 3 orders of magnitude,[7] (3) microRNA species can differ by as little as a single nucleotide,[4,5] and (4) so-called "mature" microRNA species must be distinguished from "precursors" sharing the full mature sequence.[4,5]

Given these constraints, a clinically-viable microRNA detection assay will require picomolar or better sensitivity (e.g., assuming 10 000 cells, or approximately 100 ng of total RNA, as the starting sample), greater than 3 orders of magnitude dynamic range, and single-nucleotide specificity, in addition, the quantification and delivery of an answer in a relatively short amount of time. Currently, sensitive microRNA detection is typically performed with qPCR, which boasts near-single-molecule sensitivity, high selectivity, and 10^7-fold dynamic range.[7] However, PCR amplification also has well-known drawbacks: it is sensitive to contamination, offers inaccurate quantification (limited to 2- to 4-fold changes in expression), requires validated internal reference genes, and is not easily automated for use in clinical settings.[4,5,8−10] In contrast, traditional northern blotting is highly-quantitative yet takes days to complete and requires large amounts of sample (~10 μg of total RNA or approximately 10^6 cells).[4] Microarrays are capable of a large degree of multiplexing, absolute quantification, and high sensitivity (in the 1 fg range) but require incubation for hours or days to achieve these limits.[11−13] Sequencing is emerging as a unique platform for small RNA discovery but is ill-suited to diagnostics because it is sample-hungry, requires expensive equipment and reagents, and can take up to 2 weeks to complete.[5] We previously employed molecular beacons and ITP for NA detection and demonstrated rapid (~2 min), accurate assays capable of absolute quantification.[14,15] However, molecular beacons-based assays are limited to about 100-fold dynamic range and 100 pM sensitivity due to significant background signal associated with quenching inefficiencies.[4]

We here present an assay that integrates ITP-aided hybridization with a functionalized hydrogel matrix to overcome these drawbacks. ITP is an electrokinetic focusing technique that utilizes a heterogeneous buffer system, composed of a leading (LE) and trailing electrolyte (TE), to

Received: June 9, 2012
Accepted: June 28, 2012

   dx.doi.org/10.1021/ac301586q | *Anal. Chem.* XXXX, XXX, XXX−XXX

achieve up to million-fold preconcentration in about 2 min.[16] We use ITP preconcentration to enhance hybridization of target microRNA molecules with fluorescently labeled oligos we refer to as reporters (Figure 1A).[17] We then migrate the ITP

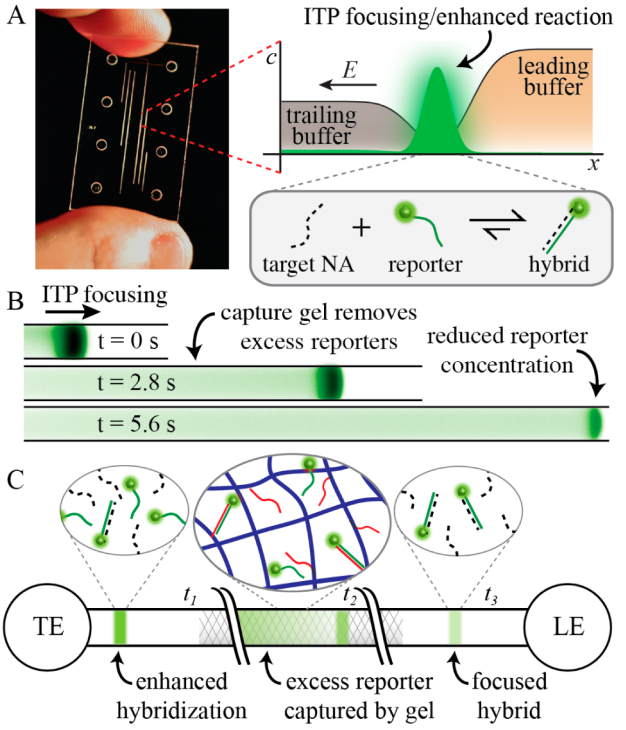

Figure 1. Integration of on-chip ITP and affinity hydrogel enables sensitive NA detection. (A) Schematic of ITP-based hybridization enhancement. ITP enables rapid mixing and approximately 10 000-fold preconcentration of NAs and fluorescent reporters in a picoliter volume. Preconcentration drives forward the reaction between target and reporter molecules, dramatically decreasing hybridization time. (B) Experimental images demonstrating ITP hydrogel capture. The ITP-focused fluorescent oligo migrates through the hydrogel, which is functionalized with probes complementary to reporters. Thus, the capture gel continuously immobilizes unreacted reporter molecules. After the ITP zone sweeps by, we observe a weak fluorescent signal left behind in the gel, corresponding to captured unused probes. (C) Schematic of microRNA detection assay. ITP in a polyacrylamide gel (upstream of the photopatterned capture gel) preconcentrates and mixes target and reporter molecules, speeding up hybridization. The ITP zone then migrates into and through the capture gel region, which removes unhybridized reporters from the focused ITP zone. This allows minimal-background detection of reporters which have specifically hybridized to their complementary target microRNA.

zone through a DNA-functionalized hydrogel where unreacted reporters are removed through affinity interactions (Figure 1B). Following the functional gel region, the concentration of unreacted fluorescent probes is mimimized, significantly reducing background signal.

Our technique addresses three out of the four main challenges posed by microRNA detection. Namely, our assay exhibits 4 orders of magnitude dynamic range, limit of detection (LOD) on the order of 1 pM, and selectivity for mature microRNAs, all achieved in less than 10 min. Additionally, our assay performs accurate absolute quantification of microRNA expression. While we do not here address assay specificity, we will further develop and demonstrate the stringency of our assay as part of future work.

In the first stage of our assay, ITP focusing simultaneously mixes and preconcentrates molecules to promote fast hybridization kinetics between target microRNAs and reporters (Figure 1C). We use only the simplest reporter molecule design: fully complementary, terminal-labeled synthetic oligos. This simplicity in reporter design enables easy tuning of probe sequence, assay temperature, and denaturant conditions to control specificity. ITP increases the concentration of both target and reporter, thereby significantly enhancing forward reaction rates.[17] Additionally, we use a relatively high initial reporter concentration (2 nM in the TE reservoir) to further promote fast kinetics. We note that the sample and reporter injection is robust and repeatable (see the Supporting Information for details on the repeatability of the sample injection signal).

Following the enhanced hybridization region, the ITP zone enters a photopatterned hydrogel region decorated with a high concentration (order 25 μM) of immobilized DNA molecules. These immobilized oligos are complementary to the focused fluorescent reporters and therefore remove excess reporters from the focused ITP zone. Preconcentration via ITP also helps promote the reaction between reporters and immobilized oligos and so enables efficient background removal. Since off-rates are typically negligible, reporters which are already hybridized to a target microRNA continue to migrate in the sharp ITP zone. Unhybridized reporters can interact with the immobilized probes and readily become immobilized in the hydrogel matrix (Figure 1B,C). Reporters remaining focused in ITP are then detected using a light source and sensitive photodetector (see the Supporting Information for details of the experimental setup). We observed that signal intensity scales directly with concentration of target molecules (Figure 2A).

We constructed a titration curve to quantify the dynamic range of our assay. We used synthetic microRNA HSA-let-7a (let-7a) for this demonstration, as this is a well-studied microRNA with diverse research and clinical applications. Members of the let-7 family, including let-7a, are implicated in cell developmental processes, have prognostic value for postoperative lung cancer patients, and are known to play a role in cancers associated with differentiation stages.[18−20] We varied the let-7a concentration over 5 orders of magnitude, from 1.4 pM to 140 nM (Figure 2B), and used the signal enhancement ratio, $\varepsilon = (I - I_0)/I_0$, as a metric to quantify our results. Here I is the integrated fluorescence intensity (above noise floor) of the experiment peak and I_0 is the mean integrated intensity (above noise floor) of the negative control peak (i.e., background signal). We note that the enhancement ratio is directly proportional to the concentration of hybridized molecules present in the ITP zone.[14,15]

We determined that our assay dynamic range spans approximately 4 orders of magnitude. Using our two-step, react-then-capture-background approach, we achieved signal enhancement ratios of approximately 4500. This constitutes a dynamic range approximately 100-fold greater than previous ITP-based hybridization assays.[14,15] In addition, we determined the assay LOD to be approximately 2.8 pM ($P = 0.0005$), for a minimum acceptable enhancement ratio of $\varepsilon \approx 1.23$ (Figure 2C). As mentioned earlier, we do not optimize our assay for high stringency (e.g., required to differentiate let-7 family members). However, we include data showing our assay signal is insensitive to a mistmatched target microRNA (HSA-miR-15a) which forms only four base-pairs with the let-7a reporter. As shown in Figure 2C, a 140 pM concentration of let-7a

dx.doi.org/10.1021/ac301586q | Anal. Chem. XXXX, XXX, XXX−XXX

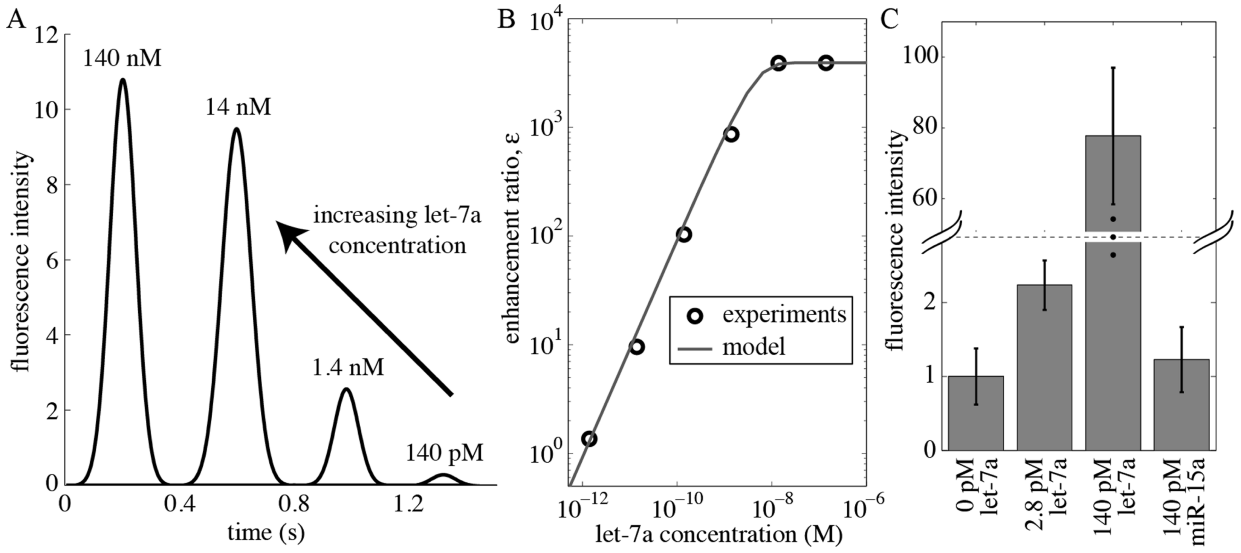

Figure 2. Experimental determination of dynamic range and sensitivity of ITP gel capture assay for detection of HSA-let-7a microRNA. (A) Gaussian best fits to measured fluorescence signal versus time for four example let-7a concentrations. Signal intensity initially scales with initial target concentration and then saturates, as predicted by our numerical model. (B) Titration curve spanning 1.4 pM to 140 nM concentrations of let-7a. The assay exhibits a quantitative dynamic range of approximately 4 orders of magnitude (with absolutely no changes in assay conditions). Shown with data is a plot of results from our model with F as a single (global) fitting parameter. (C) Limit of detection study, showing mean integrated signal intensity for negative control, 2.8 pM let-7a, 140 pM let-7a, and 140 pM of mismatch species (HSA-miR-15a). Scale bars represent 95% confidence on the mean (N = 3).

yielded an enhancement ratio $\varepsilon \approx 76.7$, while the same concentration of miR-15a yielded an enhancement ratio $\varepsilon \approx 0.2$, a value not statistically distinguishable from the negative control. Higher stringency can be achieved through use of denaturants,[11] elevated temperature,[21] and/or low salt concentration.[21] We have shown compatibility of ITP with common denaturants,[6,14] and in a future publication we explore performance of ITP analyses at elevated temperature. Higher stringency can also be achieved through the use of modified probes such as locked nucleic acid (LNA) bases, which are commonly used to lower the melting temperature of mismatched base-pairs relative to matching base-pairs.[22,23]

We model ITP-enhanced hybridization with a three-species bulk reaction model. Each species is represented by its mean concentration, c_i, where the index i stands for target (T), reporter (R), or hybrid (H) molecules. Our model is similar to the volume-averaged model proposed by Bercovici et al.[17] for DNA reactions driven by ITP mixing and focusing. The reaction equations for all three species may be written in the following form:

$$\frac{dc_H}{dt} = k_{on}c_R c_T - k_{off}c_H$$

$$\frac{dc_T}{dt} = -k_{on}c_R c_T + k_{off}c_H + Fc_{T,0}$$

$$\frac{dc_R}{dt} = -k_{on}c_R c_T + k_{off}c_H + Fc_{R,0}$$

Here t is time and k_{on} and k_{off} are the kinetic on- and off-rates, respectively. The concentrations of target and reporter molecules in the TE are $c_{T,0}$ and $c_{R,0}$, respectively. The species concentrations c_H, c_T, and c_R may be interpreted as concentrations of hybrid, target, and reporter molecules volume-averaged over the ITP zone. Similarly, the product $c_R c_T$ is volume-averaged over the ITP zone (see Bercovici et al.[17]). The single fitting parameter, F, represents the flux (per concentration) of molecules from the TE into the focused sample zone. Here we account for a semi-infinite injection mode, wherein both target and reporter molecules are mixed homogenously within the TE buffer and continuously focus into the ITP zone.[24] Experiment results are in good agreement with our numerical model (Figure 2B; see the Supporting Information for a detailed description of the numerical simulations).

We can make our assay selective for mature microRNAs by adding a second functionalized hydrogel (in series with the first) used to remove precursors from the focused zone. Precursor microRNAs contain the full mature sequence (~22 nt) within the stem of a longer (~80 nt) hairpin-shaped molecule. We functionalize this second region with DNA oligos targeting the loop sequence of precursor microRNAs, as this sequence is not present in the mature microRNA molecule. As precursor molecules enter the channel, their affinity for these immobilized probes causes them to become immobile in the hydrogel and therefore fall out of the focused ITP zone. Figure 3 summarizes experiments demonstrating the selectivity of our assay for mature microRNAs. In the presence of 140 pM precursor microRNA, our assay yields a minimal signal, which we attribute to impurities in the synthesis of the precursor molecule (resulting in some unwanted mature microRNA content in our synthesized precursor microRNA reagent; see Table S1 and Figure S5 in the Supporting Information for further details regarding oligo purity). Further, we quantified similar signals from experiments containing 140 pM of only mature microRNA versus mixtures of 140 pM of both mature and precursor microRNA. This shows that the presence of precursor let-7a in the sample does not affect quantification of mature let-7a.

In summary, we have introduced an ITP-based hybridization assay which is rapid (~10 min), sensitive (LOD of 2.8 pM), spans 4 orders of magnitude dynamic range, and is selective for

dx.doi.org/10.1021/ac301586q | Anal. Chem. XXXX, XXX, XXX−XXX

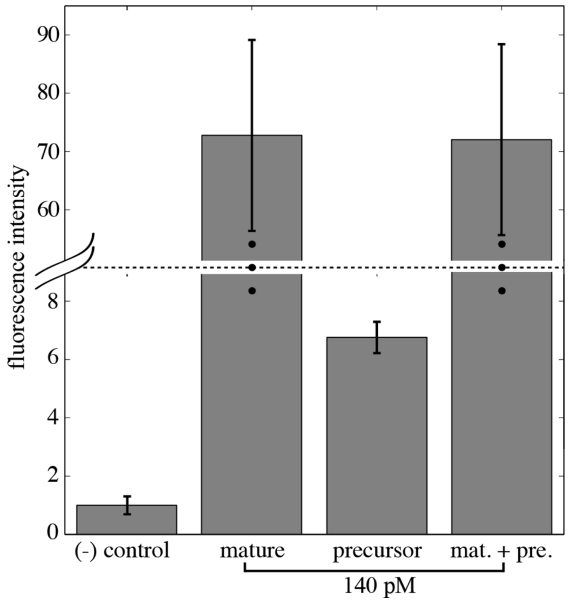

Figure 3. Demonstration of assay selectivity for mature over precursor microRNAs. For these experiments, the enhanced hybridization region contains an immobilized oligo targeting the loop sequence of the let-7a precursor (pre-let-7a) not found in the mature molecule. The plot shows mean integrated signal intensity for negative control, 140 pM let-7a, 140 pM pre-let-7a, and 140 pM each of let-7a and pre-let-7a. Scale bars represent 95% confidence on the mean (N = 3). The pure precursor sample signal is somewhat higher than the negative control signal, but we attribute this to the difficulty in synthesizing long RNA oligos of high purity. We estimate the purity of the pre-let-7a oligo is approximately 31% (see Table S1 and Figure S5 in the Supporting Information for further details regarding synthetic oligo purity).

the active (mature) form of microRNA molecules. To demonstrate our lower limit of detection, we dispensed only 300 fg of microRNA into our sample reservoir (in a 15 μL volume) and used only a small fraction of this (approximately 0.1% or about 30 000 copies) to perform our analysis. Our assay performs accurate absolute quantification, as we have shown that the measured signal is linearly proportional to the initial sample concentration. We note that our multi-stage technique does not impose limitations on probe design nor use of denaturants or temperature control. This is in contrast to one-stage techniques (e.g., using molecular beacons alone), which rely on inherent probe secondary structure for signal quenching at the cost of decreased kinetic on-rates and lower dynamic range.

In addition, we believe that our technique is generally applicable to detection of many biomolecules or reactants. For example, we hypothesize that similar strategies can be adapted for detection of proteins (e.g., using immobilized aptamers or antibodies) and other NAs. Further reduction in assay time can be achieved by increasing the applied voltage, as microfluidic systems (especially microchannels etched in glass) efficiently dissipate energy generated by Joule heating. We are adapting and extending our approach to analysis of microRNAs in total RNA samples for both research and clinical applications. We hope to further increase assay sensitivity to achieve sub-picomolar detection limits, which may enable microRNA profiling in rare cell lines. We also hope to further develop and demonstrate the stringency of our assay as part of future work.

■ ASSOCIATED CONTENT

Supporting Information

Reagents, materials, procedures, numerical simulation details, and oligo purity details. This material is available free of charge via the Internet at http://pubs.acs.org.

■ AUTHOR INFORMATION

Corresponding Author

*E-mail: juan.santiago@stanford.edu.

Notes

The authors declare no competing financial interest.

■ ACKNOWLEDGMENTS

We gratefully acknowledge funding from the Defense Advanced Research Projects Agency under Grant Number N660001-09-C-2082. G.G.-S. is supported by a Shustek Stanford Graduate Fellowship.

■ REFERENCES

(1) He, L.; Hannon, G. J. *Nat. Rev. Gen.* **2004**, *5*, 522−531.
(2) Lu, J.; Getz, G.; Miska, E. A.; Alvarez-Saavedra, E.; Lamb, J.; Peck, D.; Sweet-Cordero, A.; Ebert, B. L.; Mak, R. H.; Ferrando, A. A.; Downing, J. R.; Jacks, T.; Horvitz, H. R.; Golub, T. R. *Nature* **2005**, *435*, 834−838.
(3) Tricoli, J. V.; Jacobson, J. W. *Cancer Res.* **2007**, *67*, 4553−4555.
(4) Cissell, K. A.; Shrestha, S.; Deo, S. K. *Anal. Chem.* **2007**, *79*, 4754−4761.
(5) Baker, M. *Nat. Meth.* **2010**, *7*, 687−692.
(6) Persat, A.; Chivukula, R. R.; Mendell, J. T.; Santiago, J. G. *Anal. Chem.* **2010**, *82*, 9631−9635.
(7) Chen, C.; Ridzon, D. A.; Broomer, A. J.; Zhou, Z.; Lee, D. H.; Nguyen, J. T.; Barbisin, M.; Xu, N. L.; Mahuvakar, V. R.; Andersen, M. R.; Lao, K. Q.; Livak, K. J.; Guegler, K. J. *Nucleic Acids Res.* **2005**, *33*, e179.
(8) Corless, C. E.; Guiver, M.; Borrow, R.; Edwards-Jones, V.; Kaczmarski, E. B.; Fox, A. J. *J. Clin. Microbiol.* **2000**, *38*, 1747−1752.
(9) Bustin, S. A.; Nolan, T. *J. Biomol. Tech.* **2004**, *15*, 155−155.
(10) Benes, V.; Castoldi, M. *Methods* **2010**, *50*, 244−249.
(11) Babak, T.; Zhang, W. E. N.; Morris, Q.; Blencowe, B. J.; Hughes, T. R. *RNA* **2004**, *10*, 1813−1819.
(12) Wang, H.; Ach, R. A.; Curry, B. *RNA* **2007**, *13*, 151−159.
(13) Bissels, U.; Wild, S.; Tomiuk, S.; Holste, A.; Hafner, M.; Tuschl, T.; Bosio, A. *RNA* **2009**, *15*, 2375−2384.
(14) Persat, A.; Santiago, J. G. *Anal. Chem.* **2011**, *83*, 2310−2316.
(15) Bercovici, M.; Kaigala, G. V.; Mach, K. E.; Han, C. M.; Liao, J. C.; Santiago, J. G. *Anal. Chem.* **2011**, *83*, 4110−4117.
(16) Jung, B.; Bharadwaj, R.; Santiago, J. G. *Anal. Chem.* **2006**, *78*, 2319−2327.
(17) Bercovici, M.; Han, C. M.; Liao, J. C.; Santiago, J. G. *Proc. Natl. Acad. Sci. U.S.A.* **2012**, DOI: 10.1073/pnas.1205004109.
(18) Kloosterman, W. P.; Plasterk, R. H. A. *Dev. Cell* **2006**, *11*, 441−450.
(19) Takamizawa, J.; Konishi, H.; Yanagisawa, K.; Tomida, S.; Osada, H.; Endoh, H.; Harano, T.; Yatabe, Y.; Nagino, M.; Nimura, Y.; Mitsudomi, T.; Takahashi, T. *Cancer Res.* **2004**, *64*, 3753−3753.
(20) Shell, S.; Park, S. M.; Radjabi, A. R.; Schickel, R.; Kistner, E. O.; Jewell, D. A.; Feig, C.; Lengyel, E.; Peter, M. E. *Proc. Natl. Acad. Sci. U.S.A.* **2007**, *104*, 11400−11400.
(21) Chapin, S. C.; Appleyard, D. C.; Pregibon, D. C.; Doyle, P. S. *Angew. Chem.* **2011**, *123*, 2337−2341.
(22) Válóczi, A.; Hornyik, C.; Varga, N.; Burgyán, J.; Kauppinen, S.; Havelda, Z. *Nucleic Acids Res.* **2004**, *32*, e175.
(23) Castoldi, M.; Schmidt, S.; Benes, V.; Noerholm, M.; Kulozik, A. E.; Hentze, M. W.; Muckenthaler, M. U. *RNA* **2006**, *12*, 913−920.
(24) Khurana, T. K.; Santiago, J. G. *Anal. Chem.* **2008**, *80*, 6300−6307.